SCIENCE CHINA
Chemistry

•ARTICLES•
SPECIAL ISSUE: Celebrating the 100th Anniversary of Chemical Sciences in Nanjing University

May 2020 Vol.63 No.5: 692–698
https://doi.org/10.1007/s11426-019-9711-x

Multi-layer 3D chirality: new synthesis, AIE and computational studies

Yangxue Liu[1†], Guanzhao Wu[1,2†], Zhen Yang[2], Hossein Rouh[1], Nandakumar Katakam[1], Sultan Ahmed[1], Daniel Unruh[1], Zhonghua Cui[3,5*], Hans Lischka[1,4*] & Guigen Li[1,2*]

[1]*Department of Chemistry and Biochemistry, Texas Tech University, Lubbock, Texas 79409, USA;*
[2]*Institute of Chemistry and Biomedical Sciences, School of Chemistry and Chemical Engineering, Nanjing University, Nanjing 210093, China;*
[3]*Institute of Atomic and Molecular Physics, Jilin University, Changchun 130021, China;*
[4]*School of Pharmaceutical Sciences and Technology, Tianjin University, Tianjin 300072, China;*
[5]*Beijing National Laboratory for Molecular Sciences, Beijing 100190, China*

Received December 30, 2019; accepted February 24, 2020; published online April 2, 2020

New synthesis of multi-layer 3D chiral molecules has been developed under novel conditions to give better outcomes. The aggregation-induced emission (AIE), UV irradiation/excitation, charge transfer (CT) and local excited (LE) ππ* transitions have been investigated on a representative individual enantiomer of *pseudo* C_2 asymmetry which was made possibly by differentiating moieties on phosphorous on *N*-phosphonyl ring of chiral sandwich framework. Meanwhile, a new tandem C–N/C–C coupling reaction was unexpectedly rendered providing a novel access to special benzo[*a*]carbazoles.

multi-layer 3D chirality, organo sandwich chirality, architecture chirality, aggregation-induced emission (AIE), charge transfer (CT)

Citation: Liu Y, Wu G, Yang Z, Rouh H, Katakam N, Ahmed S, Unruh D, Cui Z, Lischka H, Li G. Multi-layer 3D chirality: new synthesis, AIE and computational studies. *Sci China Chem*, 2020, 63: 692–698, https://doi.org/10.1007/s11426-019-9711-x

1 Introduction

Chirality has attracted widespread attention in scientific communities for over a century because of its importance in chemistry, biology, material, and interdisciplines [1,2]. An increasingly large number of drugs have been showing chirality in their structures. The asymmetric synthesis and catalysis have thus become an active topic in synthesis and process chemistry in the past several decades, which heavily depend on controlling molecular chirality [3,4]. So far, the most popular and influential chirality has been represented by chiral BINAP/BINOL and C_2 symmetric scaffolds, such as vicinal chiral diols and diamines [5–10]. However, there is very limited work on conceptually new chirality of general interest and extensive potentials for chemical and biological research and material applications.

In stereochemistry, the doubly layered chirality has been established and proven to be effective in controlling asymmetric reactions [11–14]. For example, chiral titanocenes and zirconocenes have been successfully applied to asymmetric reduction/hydrogenation reactions and asymmetric polymerization processes [11]. Wilkinson ferrocene-based planar chirality has served well for asymmetric catalysis, such as Staudinger reaction, rearrangement of *O*-acylated enolates, acylation of alcohols and kinetic resolutions [13,14]. Two-layer chiral flavinium salt has been reported on the enantioselective alkyne conjugate addition and oxidation of sulfides to give modest to high enantioselectivity [15]. Very

†These authors contributed equally to this work.
*Corresponding authors (email: zcui@jlu.edu.cn; hans.lischka@univie.ac.at; guigen.li@ttu.edu)

recently, helicene dimers of two-layer chirality have been synthesized for material research; this molecular framework contains chiral elements on each wing and can be rotated to give both *syn* and *anti* stereoisomers [16].

So far, the design of multi-layer chirality and its chemical synthesis have not been well documented in literature until very recently when we became involved in this research [17]. In this work, we report the new synthesis of individual enantiomers of multi-layer chirality and organic sandwich shape (Figure 1) by performing dual C–N couplings under new catalytic systems. At the same time, we also disclose an unexpected tandem C–N coupling/cyclization reaction of 8-([1,1′-biphenyl]-4-yl)naphthalen-1-amine coupling with 1,2-dibromobenzene (Scheme 1).

As displayed in Figure 1, this new chirality shows unprecedented *pseudo* C_2 symmetry and belongs to a type of multi-layer organic framework (M-LOF) of single organic molecules. Its unique characteristics are represented by three levels of planar units arranging nearly in parallel fashion with one on top and the other one down from the centered planar anchor.

This design was initiated by our ongoing project on group-assisted purification (GAP) chemistry which is the first concept consisting of both chemical and physical aspects: reagent, reaction, separation, and purification [18,19]. By taking advantage of GAP chemistry, organic syntheses including their asymmetric versions can be conducted without the use of traditional purification by column chromatography and recrystallization. GAP functional groups can convert oily and sticky products into their solid forms, and often enable single crystals to be formed more easily when compared to classic methods. Essentially, pure GAP products can be obtained simply by washing crude mixtures with common solvents and/or co-solvents.

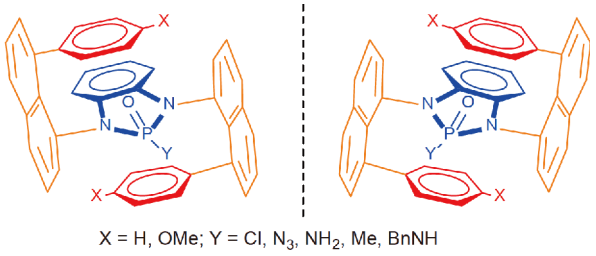

Figure 1 Multi-layer 3D chiral sandwich molecules (color online).

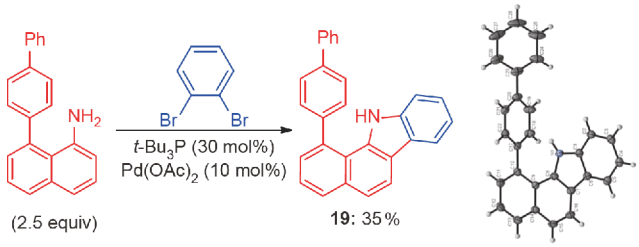

Scheme 1 Tandem catalytic C–N coupling/cyclization reaction (color online).

The search for more efficient GAP reagents has been necessitated for the following objectives: to better meet requirements of solubility, stability and reactivity of starting materials and products; to enhance diastereo-, enantio- and chemoselectivities for asymmetric synthesis and catalysis; to enable GAP protection groups to be cleaved/recycle for reuse more effectively; and to further increase chemical yields for reactions [19c]. GAP chemistry can not only avoid disadvantages for both solution-phase and solid-phase peptide synthesis, but also increase their synthetic efficiency. Moreover, it has benefited establishing solution-phase peptide synthesizer; GAP chemistry has also enabled the Fmoc protection group, which is the most popular in solid-phase peptide synthesis (SPPS), to be utilized in solution-phase peptide synthesis [19a].

2 Results and discussion

During our searching for more efficient GAP groups, we found a new single molecular framework containing multi-layered and three-dimensional chirality [17]. One of the key steps of its synthesis involves dual Buchwald-Hartwig couplings [20] of 1,2-dibromobezene with 1-amino-8-arylnaphthalene to get vicinal *N*,*N*-bis(8-arylnaphthalen-1-yl) benzene-1,2-diamines, albeit in poor yields (Scheme 2). During this synthesis, we found para-methyl anchored arylnaphthalene substrate led to the coupling product in an improved yield; and we also observed that almost all diamino precursors and multi-layer compounds are highly fluorescence-active (Figure 2; Figure S30, Supporting Information online). These findings led us to attach a stronger electron-donating group, MeO–, onto the arylnaphthalene substrate trying to further enhance chemical yields. In addition, since phenyl rings of two wings of multi-layer 3D chiral products are conjugated by –OMe group, it would result in new photoelectronic properties for future material research. However, under original catalytic systems, this replacement did not improve chemical yields that are indeed on the same level as these of previous couplings. We thus continued searching for new catalytic conditions in order to optimize the key dual couplings.

As shown in Table 1, several factors for this catalytic coupling need to be adjusted carefully. It should be mentioned that in our initial synthesis, the use of 1-bromo-8-phenylnaphthalene to react with vicinal benzene diamine did not result in any diamino product. This lesson suggested us to directly use 1,2-dibromobenzene and 8-(4-methoxyphenyl) naphthalen-1-amine as reactants for present optimizations. The coupling in toluene with 3.0 equiv. of *t*-BuONa at 110 °C only afforded 11% yield. The yield was slightly im-

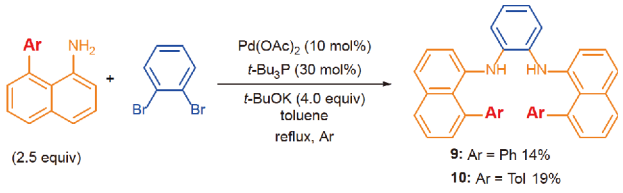

Scheme 2 Dual Buchwald-Hartwig Diamino couplings [16b] (color online).

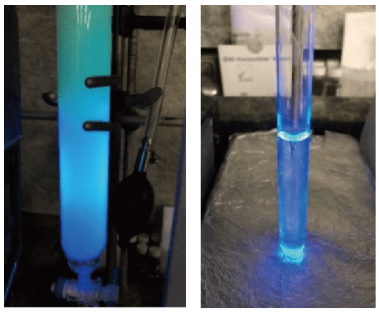

Figure 2 Fluorescence showings of multi-layer 3D chiral amide (**16a**) (color online).

proved to 15% when the reaction was performed in *p*-xylene. Replacing *t*-BuONa with *t*-BuOK resulted in a higher yield to 19%. Decreasing the loading of *t*-BuOK to 2.1 equiv. further increased chemical yield to 24%. Shortening reaction time from 24 to 19 and 14 h, chemical yields were increased to 33% and 41%, respectively (Table 1).

After achieving the above optimization, we next re-investigated the original coupling of 1,2-dibromobenzene with 1-amino-8-phenylnaphthalene under this new catalytic system. We found this system resulted in vicinal *N*,*N*-bis(8-phenylnaphthalen-1-yl)benzene-1,2-diamine in a chemical yield of 27% which almost doubled the original yield of 14% (Scheme 3). It is interesting that as shown in the X-ray structure of this diamino product, the phenyl ring on position N^1 of (8-phenylnaphthalen-1-yl)benzene 1,2-diamine is arranged in parallel to the corresponding naphthyl ring on N^2 of this benzene 1,2-diamine, and *vice versa*. However, as shown in Scheme 4, this conformation has to be adjusted to become those of **9** and **10** so as to enable the next cyclization to occur. The serious steric effects by two phenyl groups of vicinal *N*,*N*-bis(8-aryl- naphthalen-1-yl)benzene-1,2-diamines would be responsible not only for low chemical yields of dual couplings (27% and 41% for **9** and **10**, respectively), but also for relatively low yields of the next cyclization step (39% and 69% for **11** and **12**, respectively).

As shown in Schemes 4 and 5, nine steps were needed to achieve the GAP amide product of 2-amino-1,3-bis(8-(4-methoxyphenyl)naphthalen-1-yl)-1,3-dihydrobenzo[*d*][1,3,2]diazaphosphole 2-oxide (**16**). The synthesis was started from an inexpensive commercial chemical, naphthalene-1,8-diamine, via oxidative cyclization by treating with sodium nitrite in aqueous media containing acetic acid. The resulting 1*H*-naphtho[1,8-*de*][1,2,3]triazine (**2**) was treated with metal copper in hydrogen bromide to give 8-bromonaphthalen-1-amine (**3**) which was converted into *N*-(8-bromonaphthalen-1-yl)acetamide (**4**) by protection with acetyl chloride. Suzuki coupling of **4** with (4-methoxyphenyl)boronic acid gave *N*-(8-(4-methoxyphenyl)naphthalen-1-yl)acetamide (**6**) followed by acidic hydrolysis with concentrated aqueous HCl to afford 8-(4-methoxyphenyl) naphthalen-1-amine (**8**). The optimized conditions of dual Buchwald-Hartwig C–N couplings resulted in vicinal *N*,*N*-bis(8-(4-methoxyphenyl)naphthalen-1-yl)benzene-1,2-diamine (**10**) which exists in an equilibrium of enantiomeric conformers. Two of these conformers are represented, which is based on the conformations of next cyclized *N*-phosphonyl chlorides (Figure S29) and X-ray structural analysis of its derived phosphoramide. As usual, we made several efforts on obtaining these enantiomeric conformers by chiral high performance liquid chromatography (HPLC), but we fizzled due to their unfixed flexibility. However, after they are cyclized to 2-chloro-1,3-bis(8-(4-methoxyphenyl)naphthalen-1-yl)-1,3-dihydrobenzo[*d*][1,3,2]diazaphosphole 2-oxides (**12**), we were able to separate these two enantiomers via chiral prep-HPLC (Scheme 4).

At the cyclization step, the reaction of diamines with

Table 1 Palladium-catalyzed coupling conditions and results[a)]

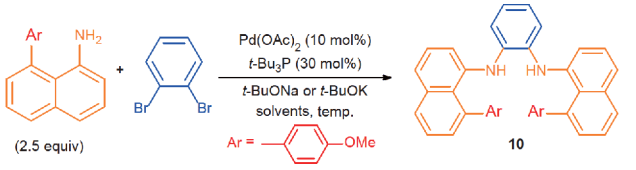

Entry	Base	Solvent	Temperature (°C)	Time (h)	Yield (%)
1	*t*-BuONa (3.0 equiv.)	toluene	110	24	11
2	*t*-BuONa (3.0 equiv.)	*p*-xylene	133	24	15
3	*t*-BuOK (3.0 equiv.)	*p*-xylene	133	24	19
4	*t*-BuOK (2.1 equiv.)	*p*-xylene	133	24	24
5	*t*-BuOK (2.1 equiv.)	*p*-xylene	133	19	33
6	*t*-BuOK (2.1 equiv.)	*p*-xylene	133	14	41

a) All reactions were performed in tubes which are tightly capped by septum and protected with balloons filled with argon gas; during the reaction, a small amount of hexane employed for preparation of $(t\text{-Bu})_3$P solution flew into balloon through needle on septum.

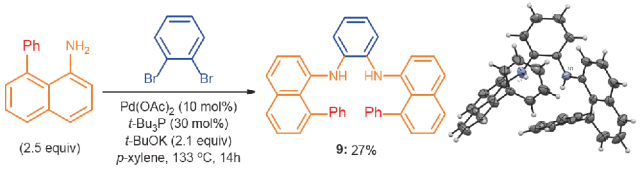

Scheme 3 Diamino coupling using 1-amino-8-phenylnaphthalene (color online).

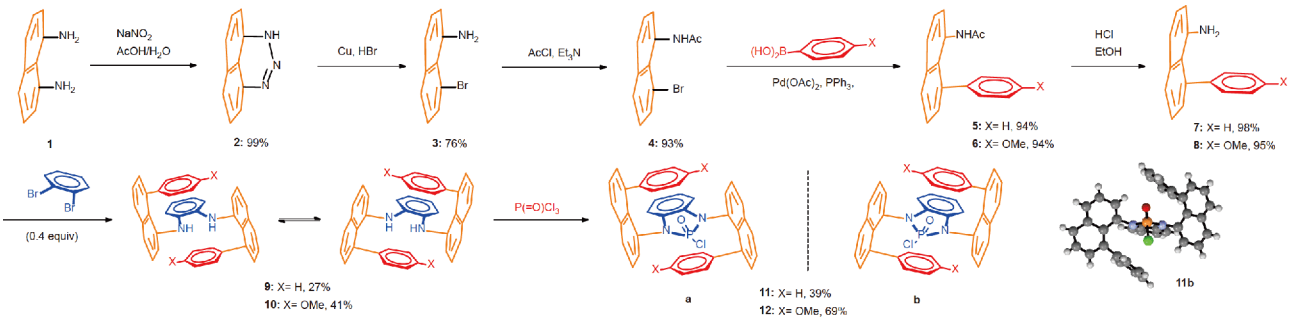

Scheme 4 Synthesis of *Pseudo* C_2 & 3D *N*,*N*-phosphonyl chlorides (color online).

phosphoryl trichloride in triethylamine or pyridine did not give any cyclization product, although they worked well for cases of (*1R*,*2R*)-cyclohexane-1,2-diamine and (*1R*,*2R*)-1,2-diphenylethane [18,19]. This reaction has to be performed by pre-deprotonating *N*,*N*-bis(8-(4-methoxyphenyl)naphthalen-1-yl)benzene-1,2-diamine (**10**) with *n*-butyl lithium followed by the treatment with phosphorus oxychloride at −78 °C in dried tetrahydrofuran (THF). In our original cyclization of *N*,*N*-bis(8-phenylnaphthalen-1-yl)benzene-1,2-diamine, a yield of 39% was obtained. However, in the present case, the corresponding yield was substantially enhanced to 69%, which is likely due to the strong-electron donating effect of the methoxy group making diamino moieties more nucleophilically reactive toward the *N*-phosphonyl protection in both intramolecular and intermolecular manners at this step. This observation is consistent with the case of the methyl derivative under the same conditions which gave a higher chemical yield of 45% than that of the unsubstituted case (39%) [19b]. The resulting azide of this *para*-methoxy case was found to be not so stable and showed complex unknown species after being isolated and stored for a short period of time at room temperature. It was thus directly subjected to Pd/C catalyzed hydrogenation with the crude azide (**14a**) to give the final product of 2-amino-1,3-bis(8-(4-methoxyphenyl)naphthalen-1-yl)-1,3-dihydrobenzo[*d*][1,3,2]diazaphosphole 2-oxide (Scheme 5). Similarly, the multi-layer 3D compounds also showed strong fluorescence activity inside column and in solution (Figure 2). **16a** was selected at random for further aggregation-induced emission (AIE) study [21]. The photoluminescence (PL) spectra of **16a** in THF/water mixture with different water fractions (f_w) and the corresponding plot of emission enhancement versus f_w demonstrate the AIE activity (Figure 3). It is non-fluorescent when dissolved in THF solution but becomes emissive at 651 nm with a 37,500 a.u. intensity when f_w=30 vol% in THF/water mixture. While more water is gradiently added (f_w=50 vol%, 70 vol% and 90 vol%), the emission intensities are significant increase to 49,500, 56,100 and 61,800, respectively.

We also made several efforts on obtaining single crystals

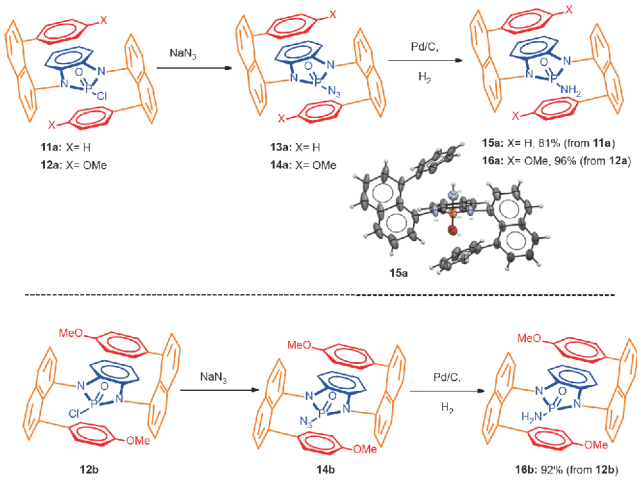

Scheme 5 Synthesis of *pseudo* C_2 & 3D *N*,*N*-phosphonyl amides (color online).

of individual enantiomers of 2-chloro-1,3-bis(8-(4-methoxyphenyl)naphthalen-1-yl)-1,3-dihydrobenzo[*d*][1,3,2]diazaphosphole 2-oxide (**12**) and the corresponding final amide product (**16**), but failed in both cases. Fortunately, the absolute stereochemistry can be assigned based on the analogous structure of 2-amino-1,3-bis(8-phenylnaphthalen-1-yl)-1,3-dihydrobenzo[*d*][1,3,2]diazaphosphole 2-oxide, which has been confirmed by X-ray diffraction analysis [19b]. The enantiomerically pure isomer of 2-chloro-1,3-bis(8-(4-methoxyphenyl)naphthalen-1-yl)-1,3-dihydrobenzo[*d*][1,3,2]diazaphosphole 2-oxide (**12b**) was further reacted with lithium benzylamine which was pre-generated by treating benzylamine with butyl lithium in THF at −78 °C (Scheme 6). The reaction was performed at −78 °C for 30 min followed by gradually increasing temperature from −78 °C to room temperature. The reaction proceeded to completion by stirring at room temperature for 6 h to give 2-(benzylamino)-1,3-bis(8-(4-methoxyphenyl)naphthalen-1-yl)-1,3-dihydrobenzo[*d*][1,3,2]diazaphosphole 2-oxide (**17**) with an 81% yield. It was also subjected to the reaction with methyl lithium under the same conditions to afford 1,3-bis(8-(4-methoxyphenyl naphthalen-1-yl)-2-methyl-1,3-dihy-

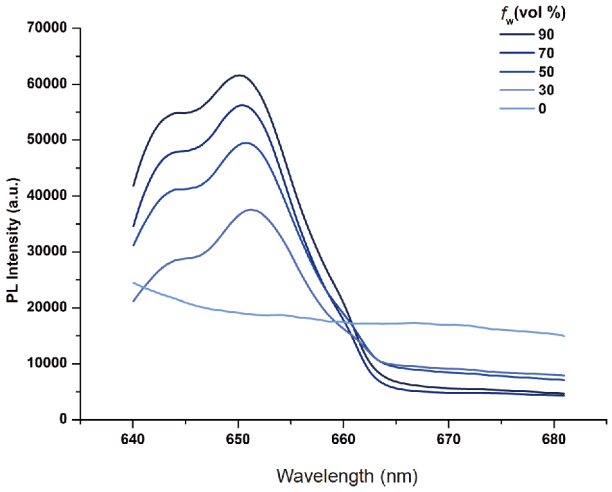

Figure 3 Photoluminescence (PL) spectra of **16a** in THF/water mixtures with different water fractions (f_w). c=1 μM; excitation wavelength (λ_{ex}): 532 nm (color online).

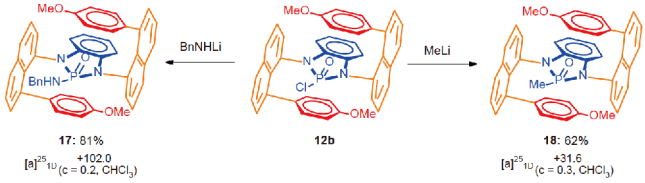

Scheme 6 Reactions of *N*,*N*-phosphonyl chloride with lithium reagents (color online).

drobenzo[*d*][1,3,2]diazaphosphole 2-oxide (**18**) in a yield of 62%. As revealed by chiral HPLC, there is no racemization observed in these two reactions.

Interestingly, when we utilized a phenyl group to replace *para* MeO– for the coupling, the reaction underwent toward another direction, i.e., intermolecular C–N bond formation was followed by intramolecular C–C cyclizing (Scheme 1). The desired product was barely formed in the resulting mixture. Instead, 1-([1,1′-biphenyl]-4-yl)-11*H*-benzo[*a*]carbazole (**19**) was generated as the major product in a 35% yield, and its structure was determined by X-ray diffraction analysis (Scheme 1). Product **19** appeared as thin snowflake-shaped solids, which benefited to generating single crystals for X-ray analysis. This product is anticipated to serve as a structural lead for material and medicinal chemistry because similar structural units showed applications in these fields [22]. As shown in its structure, the N–H bond on the indole ring is nearly perpendicular to the phenyl ring on position-8 of phenylnaphthalene; this unique arrangement will also have applications for catalyst design by introducing functional groups onto nitrogen atoms.

To further understand the electronic behavior of these new chiral molecules, we conducted computational studies by selecting **15a** as a representative model which has been unambiguously confirmed by X-ray structural analysis. In our computational methods, density functional theory (DFT) in combination with the PBE0-D3 functional [23,24] and the cc-pVDZ basis set [25] was used to optimize the geometry of the complex (Figure 4). To preserve the main features of the crystal structure, selected atoms indicated in this figure were fixed at their positions in the crystal structure during the optimization process. Second-order algebraic diagrammatic construction (ADC(2)) calculations [26–28] were performed using the TVZP basis set [29] to compute the excited-state spectrum. Natural transition orbitals (NTOs) [30] were used to characterize the electronic transition at orbital level. Environmental effects were considered by the conductor-like screening model (COSMO) [31], based on the state specific approach [32]. For the dielectric constant ε and the refractive index n, respectively, the values ε=8.93 and n=1.42 were used, which correspond to the weakly polar dichloromethane. For the calculation of the vertical emission transition from S_1, water was chosen as solvent (ε=78.4 and n=1.33). The calculations were carried out using the program package TURBOMOLE [33].

The selected bond and interring distances are displayed in Figure 4. Compared to the crystal structure, the calculated bond distances of the aromatic systems do not show significant differences, whereas the four bonds associated with the phosphorus atom are slightly longer by 0.03 Å. The two interring distances given in Figure 4 are 0.2–0.3 Å shorter than in the crystal, demonstrating the crystal packing effect on these weak nonbonded interactions.

The computed UV/Vis spectrum is displayed in Figure 5. The spectrum is characterized by two low-lying charge transfer (CT) bands at 332 and 319 nm. The CT involved in these transitions is quite significant and amounts to 0.8*e*. It is directed from the central ring to the naphthalene units (see insets in Figure 5). The location of these two weak transitions clearly indicates that the broadened absorption observed at around 320–330 nm can be ascribed to CT transitions. The next group of transitions around 280 nm are responsible for the next band and represent local excited (LE) ππ* transitions within the naphthalene ring. The strongest band is formed by a series of closely-spaced transitions between 216 to 228 nm, which are characterized as LE in naphthalene coupled with CT character. The UV/Vis spectrum predicted by ADC(2) is consistent with the experimental data (Figure S31), which shows the broadened absorption at 330 nm (CT transitions) and very pronounced absorption at around 290 nm owing to the LE transitions. The sharp absorption at around 240 nm in computed spectrum can be ascribed to the closely-spaced transitions with LE coupled with CT character.

The luminescence properties of the model **15a** structure (Figure 4) have been investigated at ADC(2) level. For that purpose, the structure of **15a** has been optimized for the S_1 state in gas phase without geometry restrictions. Structural changes in comparison to the ground state and the vertical

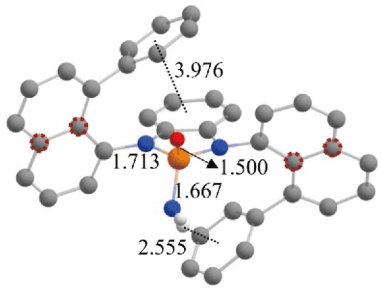

Figure 4 Optimized structures with selected bond distances in Å computed at the PBE0-D3/cc-pVDZ level. Hydrogen atoms connected to carbon are not shown and the carbon atoms fixed in the optimized process are marked by circles (color online).

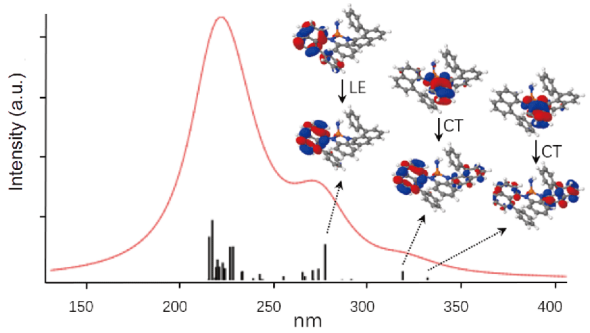

Figure 5 Simulated UV/Vis spectrum at the ADC(2)/cc-pVDZ level in dichloromethane, and pictures of the NTOs are given for S_1, S_2 (CT transitions) and S_5 (LE) states (color online).

emission energy for aqueous solution have been calculated. The CT in S_1 has the effect of equalizing the C–C bond distances in the naphthalene subunit. The C–N bond lengths in the heterocycle decrease between 0.03 and 0.05 Å. The vertical emission wavelength is computed at 594 nm for a monomer unit. The comparison of the computed emission wavelength with the experimental luminescence band maximum for **16a** at 650 (aggregated state) gives an estimate for the effect of the aggregation on the emission wavelength of about 60 nm. Moreover, a pronounced Stokes shift of 249 nm, computed as the difference of vertical excitation and emission energies in water for the non-aggregated systems, is found.

3 Conclusions

In summary, we developed more efficient synthesis of organic sandwich molecules with unique *pseudo* C_2-symmetry by searching for new dual catalytic couplings. The *pseudo* C_2 design was made possibly by differentiating two moieties on phosphorous on the centred five-membered *N*-phosphonyl ring. Meanwhile, a new catalytic reaction was established for the formation of 1-([1,1′-biphenyl]-4-yl)-11*H*-benzo[*a*]carbazole as confirmed by X-ray diffraction analysis. The AIE, UV irradiation/excitation, CT and LE ππ* transitions have been investigated on a representative individual enantiomer. We have found that the UV/vis spectrum predicted by ADC (2) is very well consistent with the experimental data, which show the broadened absorption at 330 nm (CT transitions) and very pronounced absorption at around 290 nm owing to the LE transitions. The sharp absorption at around 240 nm in experimental spectrum can be ascribed to the closely-spaced transitions with LE coupled with CT character. The comparison of the calculated emission energy for the monomer unit with the experimental band maximum for the aggregated state shows a substantial influence of the aggregation of about 60 nm.

Acknowledgements This work was supported by the National Natural Science Foundation of China (91956110, 21672100) and Robert A. Welch Foundation (D-1361, USA). Z. C. acknowledges financial support from Beijing National Laboratory for Molecular Sciences (BNLMS201910). H. L. are grateful for support from the School of Pharmaceutical Science and Technology (SPST), Tianjin University, Tianjin, China, including computer time on the SPST computer cluster Arran. We thank Dr. Kaz Surowiec for the analytic assistance discussion.

Conflict of interest The authors declare that they have no conflict of interest.

Supporting information The supporting information is available online at http://chem.scichina.com and http://link.springer.com/journal/11426. The supporting materials are published as submitted, without typesetting or editing. The responsibility for scientific accuracy and content remains entirely with the authors.

1 (a) Corey EJ, Czakó B, Kürti L. *Molecules and Medicine*. New York: John Wiley & Sons, 2012; (b) Ojima I. *Catalytic Asymmetric Synthesis*. New York: John Wiley & Sons, 2004; (c) Sherman DH, Tsukamoto S, Williams RM. *Science*, 2015, 349: 149
2 (a) Jacobsen EN, Pfaltz A, Yamamoto H. *Comprehensive Asymmetric Catalysis: Supplement 1*: *Volume 1*. New York: Springer Science & Business Media, 2003; (b) Carreira EM, Kvaerno L. *Classics in Stereoselective Synthesis*. New York: John Wiley & Sons, 2009; (c) Nicolaou KC, Snyder SA. *Classics in Total Synthesis II*. New York: Wiley Online Library, 2003; (d) Li G, Chang HT, Sharpless KB. *Angew Chem Int Ed Engl*, 1996, 35: 451–454; (e) Doyle MP. *J Org Chem*, 2006, 71: 9253–9260
3 (a) Krautwald S, Sarlah D, Schafroth MA, Carreira EM. *Science*, 2013, 340: 1065–1068; (b) MacMillan DWC. *Nature*, 2008, 455: 304–308; (c) List B. *Synlett*, 2001, 2001: 1675–1686; (d) Akiyama T. *Chem Rev*, 2007, 107: 5744–5758; (e) Zbieg JR, Yamaguchi E, McInturff EL, Krische MJ. *Science*, 2012, 336: 324–327; (f) Taggi AE, Hafez AM, Lectka T. *Acc Chem Res*, 2003, 36: 10–19
4 (a) Cao ZY, Wang X, Tan C, Zhao XL, Zhou J, Ding K. *J Am Chem Soc*, 2013, 135: 8197–8200; (b) Xie JH, Zhou QL. *Acc Chem Res*, 2008, 41: 581–593; (c) Cai Y, Liu X, Zhou P, Feng X. *J Org Chem*, 2018, 84: 1–13; (d) Yu J, Shi F, Gong LZ. *Acc Chem Res*, 2011, 44: 1156–1171; (e) Liu Y, Li W, Zhang J. *Natl Sci Rev*, 2017, 4: 326–358
5 (a) Huang XL, He L, Shao PL, Ye S. *Angew Chem Int Ed*, 2009, 48: 192–195; (b) Ye CX, Melcamu YY, Li HH, Cheng JT, Zhang TT, Ruan YP, Zheng X, Lu X, Huang PQ. *Nat Commun*, 2018, 9: 410; (c) Zhu Y, Zhang L, Luo S. *J Am Chem Soc*, 2014, 136: 14642–14645; (d) Cheng X, Lu H, Lu Z. *Nat Commun*, 2019, 10: 3549; (e) Zhang J, Zeng X, Yang L, Zhong G. *Science*, 2018, 360: 23; (f) Zhu T, Liu Y, Smetankova M, Zhuo S, Mou C, Chai H, Jin Z, Chi YR. *Angew*

Chem Int Ed, 2019, 58: 15778–15782
6 (a) Chen J, Huang Y. *Nat Commun*, 2014, 5: 3437; (b) Guo W, Wu B, Zhou X, Chen P, Wang X, Zhou YG, Liu Y, Li C. *Angew Chem Int Ed*, 2015, 54: 4522–4526; (c) Li F, Tian D, Fan Y, Lee R, Lu G, Yin Y, Qiao B, Zhao X, Xiao Z, Jiang Z. *Nat Commun*, 2019, 10: 1774; (d) Luo J, Zhang T, Wang L, Liao G, Yao Q, Wu Y, Zhan B, Lan Y, Lin X, Shi B. *Angew Chem*, 2019, 131: 6780–6784; (e) Yang G, Guo D, Meng D, Wang J. *Nat Commun*, 2019, 10: 3062; (f) Ma DK, Miao CB, Sun JW. *J Am Chem Soc*, 2019
7 (a)Zhang J, Yu P, Li SY, Sun H, Xiang SH, Wang JJ, Houk KN, Tan B. *Science,* 2018, 361: 1087; (b) Lin JS, Li TT, Jiao GY, Gu QS, Cheng JT, Lv L, Liu XY. *Angew Chem Int Ed*, 2019, 58: 7092–7096; (c) Zhang D, Qiu H, Jiang L, Lv F, Ma C, Hu W. *Angew Chem Int Ed*, 2013, 52: 13356–13360
8 (a) Shi SL, Wong ZL, Buchwald SL. *Nature*, 2016, 532: 353–356; (b) Phipps RJ, Hamilton GL, Toste FD. *Nat Chem*, 2012, 4: 603–614; (c) Gustafson JL, Lim D, Miller SJ. *Science*, 2010, 328: 1251–1255; (d) Liu H, Dagousset G, Masson G, Retailleau P, Zhu J. *J Am Chem Soc*, 2009, 131: 4598–4599; (e) Cui X, Xu X, Lu H, Zhu S, Wojtas L, Zhang XP. *J Am Chem Soc*, 2011, 133: 3304–3307; (f) Yoon H, Marchese AD, Lautens M. *J Am Chem Soc*, 2018, 140: 10950–10954; (g) Lorion MM, Maindan K, Kapdi AR, Ackermann L. *Chem Soc Rev*, 2017, 46: 7399–7420
9 (a) Kolb HC, VanNieuwenhze MS, Sharpless KB. *Chem Rev*, 1994, 94: 2483–2547; (b) Sandoval CA, Ohkuma T, Muñiz K, Noyori R. *J Am Chem Soc*, 2003, 125: 13490–13503; (c) Chen Y, Yekta S, Yudin AK. *Chem Rev*, 2003, 103: 3155–3212; (d) Zhang Z, Butt NA, Zhang W. *Chem Rev*, 2016, 116: 14769–14827; (e) Liu Y, Zhang W. *Angew Chem Int Ed*, 2013, 52: 2203–2206
10 (a) Shao X, Li K, Malcolmson SJ. *J Am Chem Soc*, 2018, 140: 7083–7087; (b) Chen D, Timmons C, Chao S, Li G. *Eur J Org Chem*, 2004, 2004(14): 3097–3101; (c) Chen D, Guo L, Liu J, Kirtane S, Cannon JF, Li G. *Org Lett*, 2005, 7: 921–924
11 (a) Jende LN, Vantomme A, Welle A, Brusson JM, Carpentier JF, Kirillov E. *J Organomet Chem*, 2018, 878: 19–29; (b) Varga V, Pinkas J, Císařová I, Kubišta J, Horáček M, Mach K, Gyepes R. *Eur J Inorg Chem*, 2018, 2018: 2637–2647
12 (a) Goodwin CAP, Ortu F, Reta D, Chilton NF, Mills DP. *Nature*, 2017, 548: 439–442; (b) Guo FS, Day BM, Chen YC, Tong ML, Mansikkamäki A, Layfield RA. *Angew Chem Int Ed*, 2017, 56: 11445–11449
13 (a) Dai LX, Tu T, You SL, Deng WP, Hou XL. *Acc Chem Res*, 2003, 36: 659–667; (b) Fu GC. *Acc Chem Res*, 2000, 33: 412–420
14 (a) Ruble JC, Fu GC. *J Am Chem Soc*, 1998, 120: 11532–11533; (b) Shintani R, Lo MMC, Fu GC. *Org Lett*, 2000, 2: 3695–3697
15 (a) Mishra S, Liu J, Aponick A. *J Am Chem Soc*, 2017, 139: 3352–3355; (b) Vyskočil Š, Meca L, Tišlerová I, Císařová I, Polášek M, Harutyunyan SR, Belokon YN, Stead RMJ, Farrugia L, Lockhart SC, Mitchell WL, Kočovský P. *Chem Eur J*, 2002, 8: 4633–4648; (c) Jurok R, Cibulka R, Dvořáková H, Hampl F, Hodačová J. *Eur J Org Chem*, 2010, 2010: 5217–5224
16 (a) Klívar J, Šámal M, Jančařík A, Vacek J, Bednárová L, Buděšínský M, Fiedler P, Starý I, Stará IG. *Eur J Org Chem*, 2018, 37: 5164–5178; (b) Isla H, Srebro-Hooper M, Jean M, Vanthuyne N, Roisnel T, Lunkley JL, Muller G, Williams JAG, Autschbach J, Crassous J. *Chem Commun*, 2016, 52: 5932–5935
17 (a) The first X-ray structure of racemic multi-layered framework was achieved in our lab by one of us (DU) on April 24, 2018 as proven by the original database; (b) Wu G, Liu Y, Yang Z, Katakam N, Rouh H, Ahmed S, Unruh D, Surowiec K, Li G. *Research*, 2019, 2019: 1–11; (c) Wu G, Liu Y, Yang Z, Jiang T, Katakam N, Rouh H, Ma L, Tang Y, Ahmed S, Rahman AU, Huang H, Unruh D, Li G. *Natl Sci Rev*, 2019, https://doi.org/10.1093/nsr/nwz203
18 (a) An G, Seifert C, Li G. *Org Biomol Chem*, 2015, 13: 1600–1617; (b) Xie JB, Luo J, Winn TR, Cordes DB, Li G. *Beilstein J Org Chem*, 2014, 10: 746–751; (c) Kaur P, Wever W, Pindi S, Milles R, Gu P, Shi M, Li G. *Green Chem*, 2011, 13: 1288–1292
19 (a) Seifert CW, Paniagua A, White GA, Cai L, Li G. *Eur J Org Chem*, 2016, 2016: 1714–1719; (b) Kaur P, Pindi S, Wever W, Rajale T, Li G. *J Org Chem*, 2010, 75: 5144–5150; (c) Seifert CW. *Dissertation for the Doctoral Degree*. Lubbock: Texas Tech University, 2017
20 (a) Guram AS, Buchwald SL. *J Am Chem Soc*, 1994, 116: 7901–7902; (b) Paul F, Patt J, Hartwig JF. *J Am Chem Soc*, 1994, 116: 5969–5970; (c) Bhunia S, Pawar GG, Kumar SV, Jiang Y, Ma D. *Angew Chem Int Ed*, 2017, 56: 16136–16179
21 (a) Hu X, Zhao X, He B, Zhao Z, Zheng Z, Zhang P, Shi X, Kwok RTK, Lam JWY, Qin A, Tang BZ. *Research*, 2018, 2018: 3152870; (b) Huang G, Wen R, Wang Z, Li BS, Tang BZ. *Mater Chem Front*, 2018, 2: 1884–1892; (c) He B, Nie H, Chen L, Lou X, Hu R, Qin A, Zhao Z, Tang BZ. *Org Lett*, 2015, 17: 6174–6177; (d) Chen L, Wang YH, He B, Nie H, Hu R, Huang F, Qin A, Zhou XS, Zhao Z, Tang BZ. *Angew Chem Int Ed*, 2015, 54: 4231–4235; (e) Zhao Z, He B, Nie H, Chen B, Lu P, Qin A, Tang BZ. *Chem Commun*, 2014, 50: 1131–1133.
22 (a) Singh S, Samineni R, Pabbaraja S, Mehta G. *Angew Chem Int Ed*, 2018, 57: 16847–16851; (b) Sankar E, Karunakaran J, Dhivyapirabha L, Mohanakrishnan AK. *ChemistrySelect*, 2017, 2: 7899–7903
23 Adamo C, Barone V. *J Chem Phys*, 1999, 110: 6158–6170
24 Grimme S, Antony J, Ehrlich S, Krieg H. *J Chem Phys*, 2010, 132: 154104
25 Dunning TH Jr. *J Chem Phys*, 1989, 90: 1007–1023
26 Schirmer J. *Phys Rev A*, 1982, 26: 2395–2416
27 Trofimov AB, Schirmer J. *J Phys B-At Mol Opt Phys*, 1995, 28: 2299–2324
28 Hattig C, Weigend F. *J Chem Phys*, 2000, 113: 5154–5161
29 Schäfer A, Huber C, Ahlrichs R. *J Chem Phys*, 1994, 100: 5829–5835
30 Martin RL. *J Chem Phys*, 2003, 118: 4775–4777
31 Klamt A, Jonas V. *J Chem Phys*, 1996, 105: 9972–9981
32 Lunkenheimer B, Köhn A. *J Chem Theor Comput*, 2012, 9: 977–994
33 Ahlrichs R, Bär M, Häser M, Horn H, Kölmel C. *Chem Phys Lett*, 1989, 162: 165–169